TRABAJO DE FIN DE GRADO:

Utilización de técnicas de luminiscencia en el análisis de sedimentos arqueológicos

Julio 2017

Presentado por:
Nast Acosta García

Tutorizado por:
Carolina Mallol Duque
Inocencio Rafael Martín Benenzuela

Grado en Física
Universidad de La Laguna

CONTENTS

1 Abstract 2

2 Objetives 3

3 Introduction 4

3.1 State of the art 9

4 Methodology 14

4.1 Experimental procedures 14

4.1.1 Samples 14

4.1.2 Emission spectra 16

4.1.3 Absorption spectra 17

4.1.4 Time resolved spectra 17

4.2 Theoretical background 20

4.2.1 Probabilities of radiative and non-radiative transitions 20

4.2.2 Lifetime of an excited level 22

5 Results 24

5.1 Pure resin absorption and emission spectra 24

5.2 Comparison of the emission spectra and average lifetimes obtained in reference samples 26

5.3 Chicken bone emission spectra and average lifetimes as a function of burning temperature 34

5.4 Time resolved spectroscopy 38

6 Conclusions 40

6.1 Outlook 41

7 References 42

1 ABSTRACT

La aplicación de técnicas de luminiscencia en el análisis de láminas delgadas y bloques de sedimento arqueológico tiene un gran potencial de cara a la identificación de restos biológicos, como huesos, dientes o coprolitos (excrementos fosilizados). Sin embargo, es un método que se encuentra en fase de desarrollo y su realización se limita al análisis superficial y cualitativo.

El principal componente fluorescente de los huesos, dientes y coprolitos, la hidroxiapatita, es un biomineral de gran interés para la física, química, biología, arqueología e incluso la medicina. Entre sus diversas aplicaciones se encuentran la utilización como componente principal en la fabricación de lámparas fluorescentes, la detección y clasificación de minerales y elementos utilizando técnicas de luminiscencia, la utilización como componente fundamental en el desarrollo de prótesis médicas y la detección de caries en el esmalte dental.

El proceso de preparación de las láminas delgadas de sedimento arqueológico es de especial interés debido a sus consecuencias en el posterior análisis de las mismas. En primer lugar, los especímenes a estudiar deben ser secados. A continuación, son impregnados con una mezcla de resina sin acelerar, estireno y un catalizador (MEKP). Finalmente, cuando la resina solidifica consolidando las muestras, éstas son cortadas en finas secciones de 1 mm de grosor, montadas en un vidrio y adelgazadas a un grosor de 30 µm. El hecho de que la resina de preparación utilizada posea propiedades luminiscentes hace que el análisis de la luminiscencia de las muestras acarree un grado de dificultad adicional, encontrándose superpuestas las emisiones de ambas partes. Esto incita a desarrollar la búsqueda de nuevos compuestos para la fabricación de resinas no fluorescentes, o bien métodos que sean capaces de distinguir entre ambas emisiones. Es por ello que las técnicas de espectroscopía resuelta en el tiempo ganan especial interés.

Por otra parte, la importancia del efecto del fuego en diversas muestras arqueológicas, procedentes de hogueras prehistóricas, nos motiva a estudiar los efectos de la termoalteración a diferentes temperaturas en las propiedades fluorescentes del hueso.

2 OBJETIVES

Los objetivos principales de este trabajo experimental son: 1) estudiar el espectro de absorción y emisión de la resina de preparación; 2) clasificar muestras de referencia de huesos y coprolitos con base a sus características de luminiscencia; 3) analizar los espectros de emisión de una muestra de hueso termoalterado en función de diversas temperaturas de combustión y 4) aplicar técnicas de espectroscopía resuelta en tiempo para la caracterización de dichas muestras.

The main objective of this experimental research is to analyse the luminescence properties of archaeological bone and coprolite samples. In particular, this work aims to accomplish the following tasks:

- To analyse the effects of the sediment thin section manufacture process on the luminescence properties of different kinds of samples.
- To study the luminescence of the resin used in the sediment thin section manufacture process and evaluate its effect on the sample's overall luminescence emission.
- To compare the luminescence emission and average lifetimes of reference bone and coprolite samples and assess their degree of differentiation.
- To apply time resolved spectroscopy in the analysis of cow coprolite sample emission spectra.
- To determine the effect of heat alteration in the luminescence properties of bones.

3 INTRODUCTION

La utilización de técnicas de luminiscencia para analizar sedimentos arqueológicos es una interesante aplicación de gran utilidad para identificar componentes biológicos como huesos y coprolitos en las muestras sedimentarias. No obstante, se encuentra en un estado de desarrollo y análisis cualitativo, siendo de urgente necesidad el estudio a un nivel más profundo. El principal componente fluorescente de huesos, dientes y coprolitos, la hidroxiapatita, es un mineral de gran importancia para la física, la química, la arqueología e incluso la medicina. Entre sus diversas aplicaciones se encuentran la utilización como componente principal en la fabricación de lámparas fluorescentes, la detección y clasificación de minerales y elementos utilizando técnicas de luminiscencia, la utilización como componente fundamental en el desarrollo de prótesis médicas y la detección de caries en el esmalte dental. Todo ello hace que el estudio de las propiedades fluorescentes de huesos y coprolitos, debidas fundamentalmente a la hidroxiapatita, sea de especial interés bajo el punto de vista de la física aplicada, y especialmente en su utilización en ciencias arqueológicas.

Some compounds, when excited with a particular short-wavelength radiation, emit light with a wavelength of smaller energy. This physical phenomenon is called luminescence. There are two kinds of luminescence:

Phosphorescence. When the excitation radiation has been stopped and emission of radiation continues.

Fluorescence. When the radiation of light by the sample only persists if the excitation radiation continues.

In fact, the difference between both kinds is the lifetime of the luminescence, that is to say, the time during which there is luminescence after excitation has been stopped.

In addition there are two types of fluorescence that are important for the earth sciences:

Primary Fluorescence or Autofluorescence. The sample can produce fluorescence because of its natural chemical and physical composition. The most famous examples are fluorite, calcite, gypsum and autunite.

Secondary Fluorescence. In this case, the materials are stained with fluorescent dyes of interest, called fluorochromes, and then will exhibit secondary fluorescence when irradiated with a specific wavelength. Numerous applications of this technique are normally used in biological material studies, although non-biological material such as clays can be stained by fluorochromes too.

The most representative examples of fluorescent minerals are some phosphates, especially apatite, and some carbonates. Bones, mainly due to their phosphate component fluorapatite, give a strong primary fluorescence in greenish yellow when excited with blue light and a light blue fluorescence in UV light, depending on age and preservation state [1]. Soil carbonates usually radiates a bluish colour in ultraviolet-oblique incident light (UV-OIL), and a yellow colour in blue OIL [2]. The intensity of emission is a function of different parameters like impurities, e.g., organic inclusions or numerous apatite-containing substances. Samples from archaeological contexts are frequently altered by burning, which may reduce their fluorescence in a considerable way [3].

One of the most important problems in the application of luminescence techniques in soil micromorphology (the study of sediment thin sections) is that polyester resins that are normally used for the impregnation and hardening of soil samples are, - perhaps due to industrial bulk production-, somehow fluorescent. This problem becomes more accentuated due the fact that incomplete polymeration, e.g. in contact with oxygen, may create a rather strong fluorescence, which is visible around the cover slip [3].

The fluorescence of bones, teeth and coprolites is principally due their inorganic constituent known as apatite. Apatite is an interesting mineral because of its several applications in industrial and scientific fields. Aggregates of this mineral group are the main raw materials in the production of phosphorus fertilizers, fodder and technical phosphates, elementary phosphorus, and phosphor-organic compounds. This inorganic

material is often substantially enriched in rare-earth elements making its extraction possible. Detection and identification of this mineral in rocks, ores, and outcrops using luminescent Lidar (Light Detection and Ranging) technique is also a useful application of this fluorescent compound. The synthetic halo-apatite was one of the first phosphors applied for fluorescent lamps, another example of the advantage of its luminescent properties. The fluorescence of this inorganic mineral permits to establish genetic relationships between mineral samples and their source (mantle or earth's crust) and the type of rock. A correct utilization of luminescence sorting is able to enrichment apatite ores. Synthetic apatite mineral active by $Yb^{3+}$and $Mn^{5+}$are frequently used as potential laser principal materials [4].

In spite of the existence of different optical colour apatites, their physical origin is ambiguous. Recent scientific studies show that the violet-blue colour is connected with the optical broad absorption band of the SO_3^- radical, which is a result of the introduction of S and U(Th) elements in the mineral structure. The same models claim that the reason for the blue colour in apatite is due to the substitution of P^{5+} by the element Mn^{5+}. On the other hand, the explanation of the existence of the green coloured mineral apatite is based on the complex defect $SO_3 - TR(Ce)$, however the influence of Pr, Nd, Cr and Fe is also possible [4].

Because of the properties of its nucleus, the apatite mineral is considered as a good wall that prevents the leakage of radioactive nuclei from radioactive waste storage. The similarity in the chemical and spectral features makes rare-earth elements a reasonable model of the fission products of the actinides and so it is of importance to understand if the elements are incorporated in the bulk of the barrier, or adsorbed on the surface where they can be subjected to leaching.

The ideal chemical formula to express fluorapatite is $Ca_{10}(PO_4)_6F_2$. Its structure is hexagonal, with the symmetry group P63/m. For the element Ca_2 there are two positions in the crystal structure: 40% of Ca^{2+} ions are related with the Ca(I) sites and 60% are associated with Ca(II) locations. Each Ca^{2+} ion related to Ca(I) is surrounded by six oxygen molecules, forming a distorted triangular prism. On the other

hand, the Ca(II) location ions are sitting at the corners of equilateral triangles with an F^- ion in the centre as shown in Fig. 1 [4].

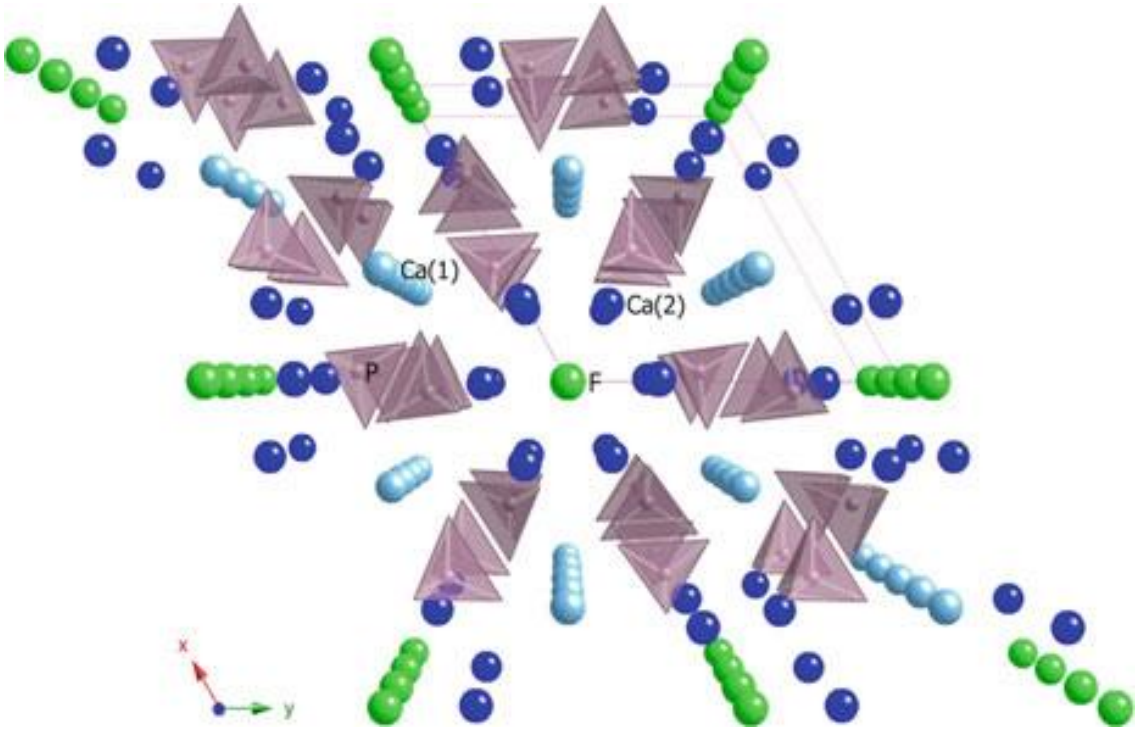

Figure 1. Apatite crystal lattice representation. The dark blue spheres represent Ca(II) ion locations, while the soft blue ones represent Ca(I). On the other hand, the green spheres represent the F locations and the grey pyramids represents PO_4 molecules locations. The primitive cell is delimited by red continuous lines [4].

Speaking more properly, the fluorescence mineral in the structure of teeth and bones is hydroxyapatite. Its chemical theoretical formula is $Ca_5(PO_4)_3OH$. It is known as a non-stoichiometric apatite, because its chemical formula is a function of the presence of different ions in very small or in trace amounts, and it has a stochastic character. These foreign ions have a great effect on the chemical and physical properties of biological apatite. Trace elements also affect the mineralization and dissolution process of biominerals, teeth and bones. An interesting and important investigation is about the effect of trace ions in hydroxyapatite such as in bone implants or as coating material for Ti or other implants. In this example, the amounts of foreign elements can have consequences on the stability of the implant, the chemical interaction at the bone-

implant interface or mechanical properties. In the case of preparation of mineral hydroxyapatite with ion traces, it is of special importance whether foreign elements can substitute Ca^{2+} in one of its crystallographic sites in the crystal lattice. In this respect, the most important factors are the size of the ions, their chemical properties and the preparation conditions [4].

Coprolites, which are fossilized excrements, are also interesting, frequent, apatite-rich archaeological samples. Like bones and teeth, their main fluorescent compound is hydroxyapatite. Their identification is important to establish the presence of particular animals in archaeological contexts. Also, they can provide an important window into the diets and digestive systems of the producing animals. In carnivorous animals, an important factor is the dietary load of calcium and phosphate, mainly acquired from bone ingestion. Most of these compounds appear as a microcrystalline apatite slurry that, with further crystallization, give structural strength after the deposition of the feces [5]. Several studies about the importance of apatite precipitation in phosphatic coprolites preservation was been carried out. Fast mineralization processes can preserve coprolites and some of their microstructures.

A significant fact that affects in a decisive way and should be taken into account in the application of luminescence techniques on archaeological research is the process of preparation of the samples to study. The fact that the resin, used to impregnate the studied samples before the preparation of the thin sections, produces considerable luminescence in the wavelength range of study, suggests that caution should be taken in sample processing and alternative impregnation methods should be sought.

The preparation of archaeological samples is an important standardized process in soil micromorphology. Due to the fragility and unconsolidated state of the soil samples collected from archaeological sites, their processing becomes a decisive factor that can prevent the damage and even the destruction of the sample. Most processed sediment blocks are to be made into thin sections and analysed through microscopy techniques. The first step of preparation consists in drying the sediment samples at 60 ºC for three to four days. After that, they are impregned with a mixture of unsaturated resin, styrene, and hardener (MEKP). Subsequently, the samples are cured for several

days, the number of days depending on function of the sample to study. Finally, the hardened blocks are cut into $7 \times 4 \times 1\ cm^3$ slabs, mounted on a large glass slide ($7\ cm \times 5\ cm \times 30\ mm$) and thinned to 30 µm.

After all their processing, usually the samples are observed under a petrographic microscope with transmitted light at 20, 40, 100, and up to 200 magnifications. The identification of sedimentary components is carried out using plane-polarized light (PPL) and crossed-polarized light (XPL). An epifluorescence module is coupled to the microscope for qualitative identification of fluorescent components such as apatite-containing particles, which are excited with blue light, or fresh organic matter, which is excited with UV light. A noteworthy fact is that the study of fluorescence is commonly carried out in a purely qualitative manner, using mere chromatic perception to identify the emission of bones and coprolites. This is a limiting factor towards the classification of fluorescent compounds, because several of them are difficult to distinguish qualitatively and the outcome is somewhat subjective.

3.1 STATE OF THE ART

Hydroxyapatite crystal is of special interest in the state of the art of diverse science researches in fields like physics, chemistry, biochemistry, biology, geology, archaeology and even medicine. Among its various applications are the use as a main component in the manufacture of fluorescent lamps, the detection and classification of minerals and elements using luminescence techniques, the identification of bones and coprolites in sedimentary samples, the use as a fundamental component in the development of medical prostheses and the detection of caries in dental enamel.

La^{3+} is of interest relate to biomineral hydroxyapatite, due of their inhibitory effect on the demineralisation of dental enamel. It is not clear this lanthanide ion presence in the crystal lattice, namely surface adsorption or lattice incorporation. With the objective to clarify it, laser-induced luminescence has been used [6]. La^{3+} is not luminescent and, in order to find out whether a rare earth ion can be incorporated in a precipitated hydroxyapatite, Gd-containing hydroxyapatite samples were prepared and

tested for their luminescence spectra. Research results suggest that, in the La-containing samples, La^{3+} is surface adsorbed and not incorporated in hydroxyapatite.

Hydroxyapatite mineral is an important compound in the application of LIBS technique (Laser-induced breakdown spectroscopy) for real time identification of carious teeth. The variations of trace matrix elements like Ca and P in hydroxyapatite crystal and the increase of non-matrix compounds can be analysed with the objective to identify carious and healthy tooth material, using pattern recognition algorithms [7]. The combination of LIBS and discrimination analysis is a useful tool for real time in vivo/in vitro caries identification during the drilling process when luminous short laser pulses create plasma.

Because of the similarity on the effective atomic number of fluorapatite and human bones and teeth, this biomineral is an important type of thermoluminescence dosimeter (TLD). In this line of research there is a readable study of diverse pre-irradiation thermal treatments, with interesting results. Tooth enamel samples in powder form were analysed through numerous experiences. Some of these aliquots were used to see the effects of different annealing temperatures at fixed annealing time and after that were irradiated about 35 Gy by beta source. On the other hand, other aliquots were annealed at 1000º C for different annealing times, and after that they were irradiated with 35 Gy. Finally, in a dose response experiment, the samples were irradiated at different higher doses at different annealing temperatures. The conclusions confirm the TL properties of fluorapatite mineral extracted from tooth enamel, and the extreme effect of sample annealing on the TL glow curve, causing a huge enhancement in the sensitization of TL peak [8].

Some investigation results of real interest are about the chemical composition, structural characteristics and luminescent properties of natural bones, commercial hydroxyapatite and collagen using EMPA, XRD, Raman spectroscopy, thermal analysis, cathodoluminescence and thermoluminescence [9]. The samples used in the analysis was a little transversal section, sized $1\times1\times1\ cm^3$ of Siberian mammoth (Mammuthus primigenius), a tiny portion of African elephant (Loxodonta africana) tusk sized $1\times2\times1\ cm^3$, powdered markertable Collagen 234184 of MERCK Co. and

Hydroxyapatite Fluka 21221 of Sigma-Aldrich Co. The structural characteristics were performed using XRD (powder method), Raman spectroscopy and thermal analysis such as differential thermal analysis (DTA) and thermogravimetry (TG). On the other hand, the luminescent properties of the natural bones, commercial hydroxyapatite and the collagen were characterized by cathodoluminescence (CL) and thermoluminescence (TL) (see Fig. 2). Through chemical analyses (EMPA) were found small amounts of rare earths, Pb, Mn, Fe, Al and F incorporated in the natural bones structure. The results confirm that double composition of hydroxyapatite and collagen in bonds provide calcium-phosphate groups together with polynuclear aromatic hydrocarbons with OH and $C = O$ groups with intra-molecular hydrogen bonds. This physical phenomenon becomes an important difficulty for dosimetry and dating evaluation using inorganic apatite and HAP (hydroxyapatite).

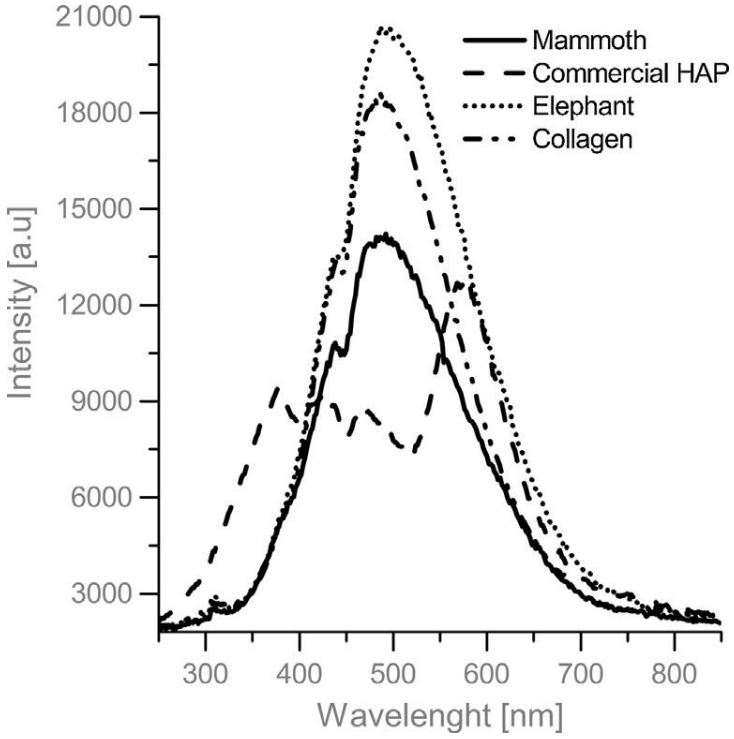

Figure 2. Emission spectra of mammoth and elephant samples, commercial HAP and collagen [9].

It is of actual importance in the application of luminescence techniques on archaeological research to understand the effect of heat on the physical and chemical properties of the materials. Significant archaeological excavations consist of numerous samples drawn from ancient bonfires, in which hominid ancestors cooked the meat and realized handicraft activities. We can divide types of heating in two groups: combustion, that is realized in presence of oxygen; and charring, that is carried out without oxygen. For both the formation of char is the first step. Through a sequence of controlled laboratory heating experiments and the application of a broad range of analytical techniques, an interesting research demonstrates that bone heated under reducing conditions shows a different thermal alteration trajectory than bone heated in the presence of oxygen [10]. Samples to study were taken from the cortical part of the femur of a mature female bovine. All these samples were charred to the required temperature, in a range from 200 to 900 ºC. After that, several physical analyses were carried out, such as TGA, reflectance analysis, XRF, CHN analysis, FTIR, Raman spectroscopy, DTMS and XRD. The results argue that in the absence of oxidation reactions the loss of organic compounds is slowed down. Because of thermal shielding, changes in the inorganic fraction of bone are delayed or prevented entirely. These findings reaffirm the importance of considering charring and combustion as two different processes, as well as highlight the importance of considering the specific heating conditions when analysing archaeological material. The results of this study show that different/additional reference data is required for the characterisation of charred bone.

In the same line of research, photothermal radiometry and diffuse reflectance were applied to study thermal and optical properties of porcine thermally treated bone, in this time, the samples were dried pig bones heated at high temperatures, in room temperature range up to 350 ºC. The samples were structurally characterized by XRD and infrared spectroscopy. The results dictate that exist an increase of thermal diffusivity and reflectance for the low-temperature range up to a maximum around 125 ºC, and then there is decay at higher temperatures. Above the mentioned temperature, the reflectance exhibits a strong decay to values much lower than the values found for samples at ambient temperature. To detect complex changes in the biogenic composition, such as dehydration, dehydroxylation, elimination of the organic material,

and removal of the fibril collagen networks, which have an influence on the bone chemical milieu and microcrystalline structural reorganization, it is shown that thermal diffusion and optical reflectance are sensitive parameters. The behaviour of the absorbance-scattering coefficient mimics the colour changes due to combustion and carbonization of the organic matter [11].

4 METHODOLOGY

En este trabajo incluimos cuatro tipos de muestras. Las primeras consisten en 5 muestras de referencia de hueso de taxón y parte anatómica conocidos. El segundo tipo consiste en una pieza pura de resina, con la que las muestras arqueológicas son preparadas. El tercer tipo lo conforman 7 muestras de referencia de coprolitos de animales conocidos. La última muestra a estudio se trata de un hueso de pollo, quemado en un rango de temperatura de 100 a 400º C. En primer lugar, se analizaron los espectros de emisión y absorción de la resina pura de preparación. Seguidamente, se compararon los espectros de emisión y tiempos de vida medios de las muestras de referencia de huesos y coprolitos y del hueso de pollo termoalterado. Finalmente, se llevaron a cabo estudios de espectroscopía resuelta en el tiempo para el caso de la muestra de referencia de coprolito de vaca.

4.1 EXPERIMENTAL PROCEDURES

4.1.1 Samples

Four types of samples were studied in this work. Two examples are shown in Fig 3.

(1) Pure resin sample. This resin is the one employed in the sediment thin sections preparation. The approximate dimensions of the sample are $1.5 \times 0.8 \times 0.3\ cm^3$. The pure resin piece was analysed with the purpose of characterizing the emission of resin and identify it in subsequent sample spectra, where the resin and bone emission spectra overlap.

(2) Reference bone samples (human and animal). These samples were analysed with the objective to find a luminescence behaviour that might help us classify them and thus identify future unknown samples. In the present study we focussed on five of these samples: ancient human tibia, modern human tibia, burned human bone, goat tibia and fish vertebra. The samples were prepared as described in the introduction, and their dimensions are $5.9 \times 4.7 \times 0.1\ cm^3$.

(3) Reference archaeological coprolites. Coprolites consist of fossilized animal excrements of special interest in archaeological science. Just like the reference bone samples, the animal that produced the coprolites was known. Seven of these samples were analysed: camel coprolite, cow coprolite, ferret coprolite, pig coprolite, two rabbit coprolites and a final sample labelled "coprolite 06" for which the animal was unknown. The approximate dimensions of the samples are $4.8 \times 2.7 \times 0.1\ cm^3$. The animal coprolites reference samples were analysed in order to characterize their fluorescence spectra towards future identification of future coprolite samples for which the animal is unknown.

(4) Modern chicken bone. A typical chicken bone, burned at 100, 200, 300 and 400º C using a laboratory furnace in oxidizing conditions (Gero 30-3000º C). The approximate dimensions of the samples are $2.2 \times 0.6 \times 0.2\ cm^3$. Each burning temperature was maintained for 30 minutes under an oxidizing atmosphere. The chicken bone emission spectra were analysed to explore the effects of burning in the fluorescence properties of bones.

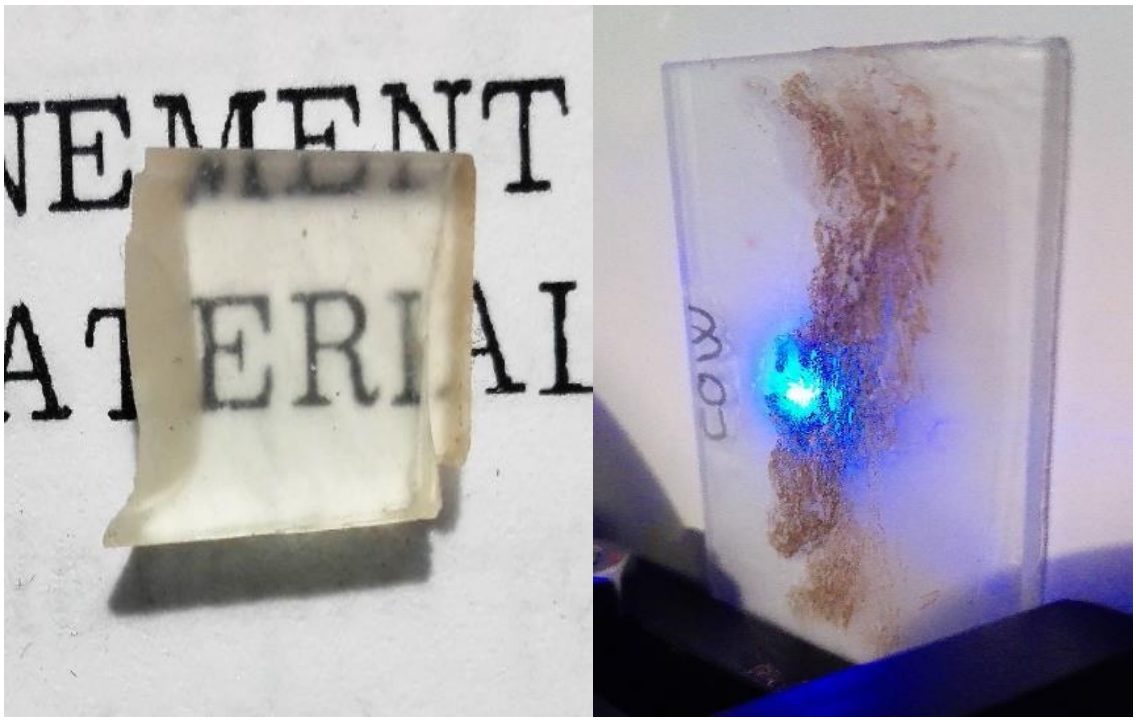

Figure 3. Two examples of studied samples: left, pure resin piece; right, cow coprolite excited at 405 nm.

4.1.2 Emission spectra

The emission spectra of the different samples were obtained using a principal setup, in which different sources of excitation have been used.

The setup is based on a 405 nm blue laser, due to its small dimensions and its economical price. Therefore, LM4020M-S1S5 405 nm Blue Light Laser Module was used. The experimental scheme is shown in Fig. 4. The collimated laser light beam is converged with a lens in order to excite a few mm of the sample. After that, the fluorescence emission of the sample goes through a convergent lens and a 435 nm long pass filter so that the laser emission is not measured by the spectrometer. The emission impinges on an optical fibre located on a vertical platform whose displacement along two axes is achieved with two micrometre screws. The optical fibre was coupled to a single grating CCD spectrometer (Andor SR-3031-B CCD Newton DU920N).

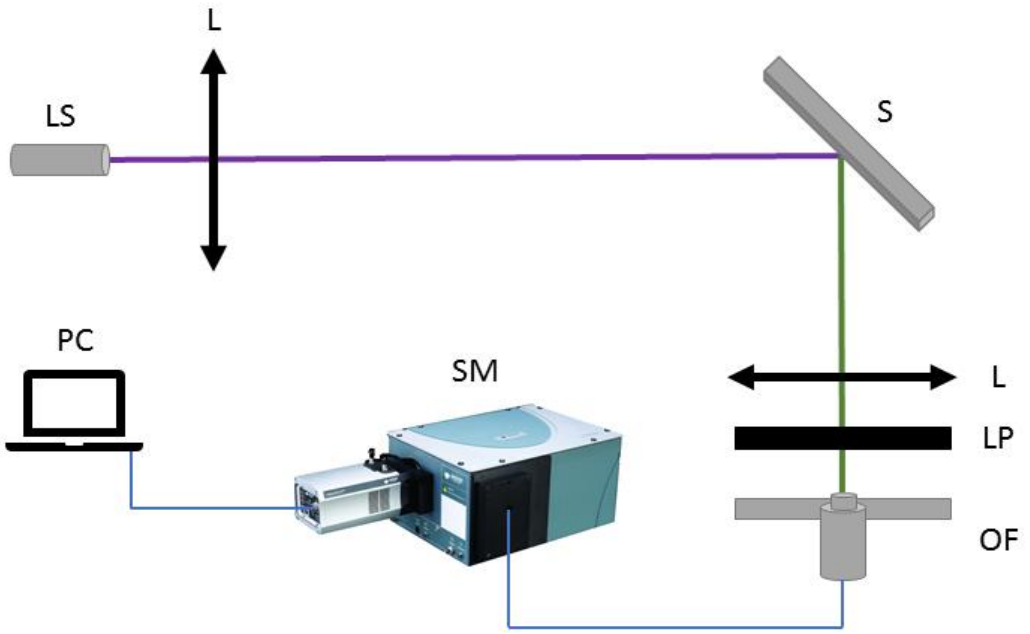

Figure 4. Experimental setup for spectral measurement. The acronym labels correspond to LS 405 nm Laser Source, L Lens, S Sample, LP 435 nm Long Pass Filter, OF Optical Fibre, SM Spectrometer and PC Personal Computer.

Although it is possible to obtain a good fluorescence signal from the sample by exciting the samples using a 405 nm laser, there is also emission from the resin. Therefore, it is convenient to look for another excitation wavelength range where the resin fluorescence becomes smaller than the bone and coprolite fluorescence.

For this reason, the excitation source at 405 nm was replaced by 380 nm laser source. In this experiment, an OPO (Optical Parametric Oscillator) laser was used to produce a 380 nm pulsed laser beam. Due to the harmonic residual emission produced by the OPO laser, a short pass filter was used. In this setup, like in the previous one, the laser beam is converged by a lens into the sample surface. After that, the fluorescence emission of the sample goes through a second converged lens and a 435 nm long pass filter. Finally, the signal is collected using an optical fibre and focused to the entrance of the Andor SR-3031-B CCD Newton DU920N spectrometer.

4.1.3 Absorption spectra

Absorption spectra measurement was carried out using an UV-Vis-NIR Spectrophotometer (Cary 5000) in the range from 200 to 1100 nm. Because of the existence of glass in the reference samples, the absorption spectrum of resin was obtained using pure resin and cut to a thickness of approximately 2.9 mm.

4.1.4 Time resolved spectra

Due to the convolution of the emission of resin and bones or coprolites, we used time resolved spectroscopy. This method facilitates the identification and separation of overlapping emission signals, on the basis that different excitation levels have different lifetimes. In this procedure, after the incidence of the laser pulse into the sample surface, when the population decay starts, the emission spectrum is measured over a specific time interval. Therefore, we obtain a spectrum in which all possible transitions from the excited state will be superimposed. After a certain delay time from the moment of excitation, the measurement is repeated. This process is represented in Fig. 5. The

obtained spectrum will be the same that the first one, but due the more advanced degree of decay of the excited levels, spectral lines of lower intensity will be obtained. Moreover, because the different emissions come from different excited states with different lifetime values, the spectral lines will decrease in different ways. In this way, we observed that with long delay times we only detect emissions coming from long lifetime excited levels.

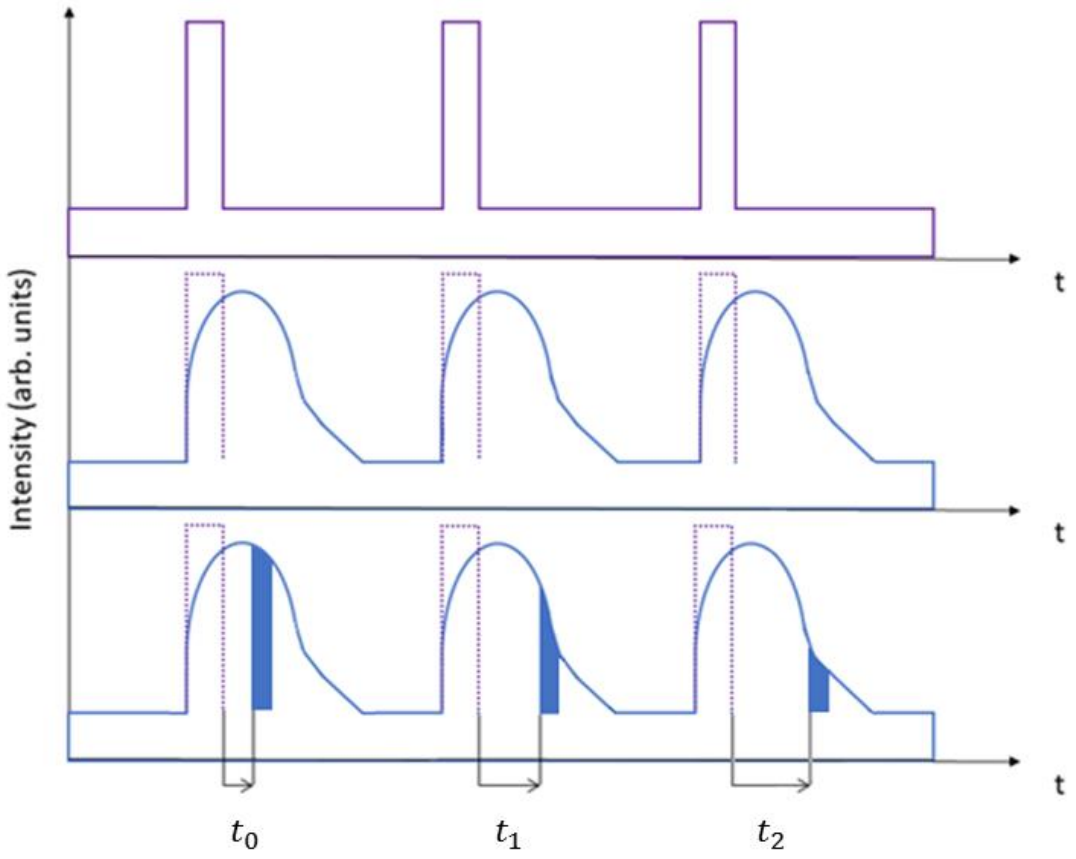

Figure 5. Time resolved spectroscopy. In the top, the excitation laser pulse; in the middle, the fluorescence emission of the sample; in the bottom, in blue, the time interval taken for the emission spectra measurement, after different values from the laser excitation.

The time resolved spectra measurements were carried out using the setup shown in Fig. 6. The OPO laser was used to produce a 380 nm pulsed laser beam. After goes through a short pass filter and a lens, the laser beam is focused in the sample surface. Next that, the emission of the sample goes through a second converged lens and a 435 nm long pass filter. Finally, the signal is collected in monochromator Triax 180 with a photomultiplier. The voltage signal is measured by a digital oscilloscope, being this one proportional to the intensity signal. On the other hand, in order to know at which instant of time the excitation pulse impacts on the sample, a photodiode detector is used. This detector is connected with the digital oscilloscope, indicating to it at which time the trigger must be activated.

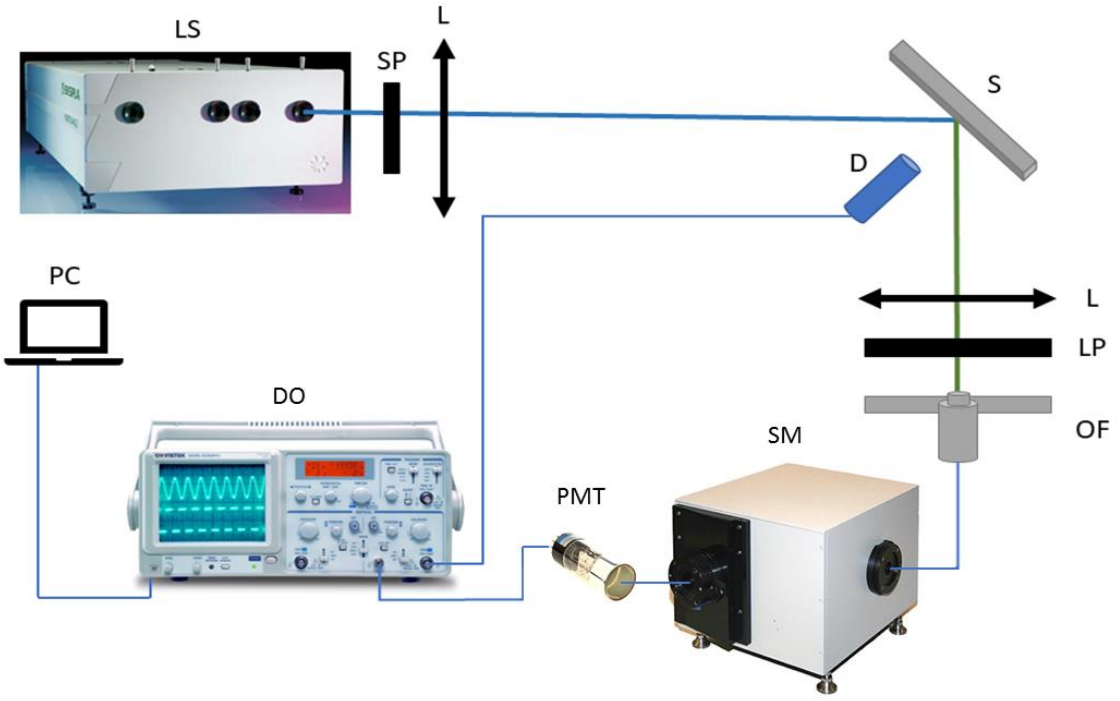

Figure 6. Time resolved spectra measurement set-up. The acronym labels correspond to LS 380 nm Pulse OPO Laser Source, SP Short Pass Filter, L Lens, S Sample, LP 435 nm Long Pass Filter, OF Optical Fibre, SM Spectrometer, PMT Photomultiplier Tube, DO Digital Oscilloscope, D Pulse Detector and PC Personal Computer.

On the other hand, with the goal of characterizing the lifetimes of the different samples, decay curves were obtained using the LifeSpec II (Edinburgh Instruments) and a picosecond pulsed diode laser at 375 nm with a period of 2 μs, and detecting at 512 nm, where the emission intensity is maximum in the analysed samples.

4.2 THEORETICAL BACKGROUND

4.2.1 Probabilities of radiative and non-radiative transitions

In general, most of the emission processes detected in the visible region correspond to electronic transitions. Therefore, with the objective to describe the physical process concerning the luminescence of the studied samples, it is necessary to introduce some simple concepts and theoretical models.

Suppose a system with two possible energy states for its electrons, E_1 and E_2, being $E_2 > E_1$. The possible radiative processes that can change the state of the electrons can be divided in first instance in three principal groups:

Induced absorption. If any electromagnetic radiation which photons with an energy $h\nu$, being h the Planck's constant, goes across the two levels system, it occurs that electrons in fundamental level E_1 could promote to the excited level E_2 if the energy of the photons is equal to the difference of energy between those levels. That is

$$\mathrm{E_2 - E_1 = h\nu} \tag{1}$$

Following the thermodynamics treatment of Einstein, the probability per unit of time that a particle passes from the fundamental to the excited level is

$$\frac{dP_{12}}{dt} = B_{12}\,\rho_\nu \tag{2}$$

where B_{12} is the Einstein coefficient of induced absorption and ρ_ν the spectral energy exciting the system.

Induced emission. In the case that in the initial configuration of the two levels system the electron is situated in the excited level, it can occur that if an electromagnetic wave falls upon the system the electron decay to the fundamental state emitting radiation. In this case, the emitted photon would be equal to the incident one.

It is possible to write, in the same way that in the previous case, that the probability per unit of time that an electron pass from the excited level to the fundamental one is given by

$$\frac{dP_{21}^{i}}{dt} = B_{21}\,\rho_{\nu} \tag{3}$$

being B_{21} the Einstein coefficient of induced emission.

Spontaneous emission. It can be possible that, in a system where the electrons are in the excited level, they could decay in a spontaneous process, emitting radiation to any special direction.

In this case, the probability of the transition per unit of time that an electron pass from the excited level to the fundamental level is

$$\frac{dP_{21}^{e}}{dt} = A_{21} \tag{4}$$

where A_{21} is the Einstein coefficient for the spontaneous emission.

Moreover, there are other processes that can produce a change in the state of the electrons but without intervention of photons. These processes are called nonradiative and in our experiments the most important ones are the followings:

i) **Multiphononic desexcitation:** It is possible that the electrons in an excited level decay but without emission of radiation. In this process are emitted phonons, which ones correspond to vibrational normal modes of the crystal lattice.

ii) **Nonradiative energy transfer:** Assuming two systems, it is possible that due to an electric multipolar interaction between an excited electron and the other one in the ground state, these ones could change their states. The probability of this process is inversely proportional to the distance between the donor and acceptor electrons and can be expressed as

$$W_{TE} = \frac{constant}{R^{S}} \tag{5}$$

where R is the distance between the donor and acceptor ions and S is a constant with a value equal to 6, 8 or 10, depending of the character of the interaction of the transfer process.

4.2.2 Lifetime of an excited level

Let's analyse the time evolution of a system, it is assumed N_2 electrons in the excited level and N_1 in the fundamental energy level. The variation as function of the time of the number of electrons in the excited level should is given by

$$\frac{dN_2}{dt} = -B_{21}\rho_\nu N_2 - A_{21}N_2 - W_{NR}N_2 - W_{TE}N_2 + B_{12}\rho_\nu N_1 \quad (6)$$

where W_{NR} is the probability of the multiphononic desexcitation.

Now, if the excitation source is cut off, then

$$\frac{dN_2}{dt} = -(A_{21} + W)N_2 \quad (7)$$

where $W = W_{NR} + W_{TE}$.

It is easy to integrate equation (7), giving the following result

$$N_2(t) = N_2(t = 0)e^{-t(A_{21}+W)} \quad (8)$$

Therefore, the lifetime of the excited level is defined as

$$\tau = \frac{1}{A_{21} + W} \quad (9)$$

On the other hand, apart from the above mentioned processes, other interactions, i.e., ligand to ligand and ligand to metal interactions, contribute to the decay of the fluorescence in most of the solid samples, producing a non-exponential character of decay [12]. With the objective to give an estimation of the lifetime, it is defined an average lifetime value of the fluorescence. Therefore, the decay curves are fitted to a double exponential function, in the following way

$$I(T) = B_1 e^{-\frac{t}{\tau_1}} + B_2 e^{-\frac{t}{\tau_2}} \tag{10}$$

and finally, the average lifetime [13] is calculated using

$$\tau_{av} = \frac{(B_1\tau_1^2 + B_2\tau_2^2)}{(B_1\tau_1 + B_2\tau_2)} \tag{11}$$

5 RESULTS

Las muestras de sedimentos están impregnadas en resina para su posterior estudio. Es por ello que este estudio comenzó analizando el espectro de absorción de la resina en el que se demuestra que absorbe radiación del rango UV, siendo transparente en el rango visible. Su emisión fluorescente centrada en 500 nm hace que la aplicación de técnicas de luminiscencia para el análisis de sedimentos arqueológicos obtenga un grado de dificultad adicional, siendo de gran importancia la búsqueda de nuevas resinas no fluorescentes. Por otro lado, la comparación de espectros de emisión de las muestras estándar refleja en algunos casos características intrínsecas de los especímenes, siendo posible su identificación. De la misma forma la comparación de los tiempos de vida promedios de las muestras estándar muestra un enorme potencial para la identificación de huesos y coprolitos. Finalmente, la utilización de técnicas de espectroscopía resuelta en el tiempo hace posible la separación de emisiones solapadas en la emisión espectral, resultado de gran transcendencia teniendo en cuenta que la resina de preparación es fluorescente.

5.1 PURE RESIN ABSORPTION AND EMISSION SPECTRA

The absorption spectrum of the resin is shown in Fig. 7. As we can see, there is a high absorption in the UV range but it is transparent in the visible range, fact that favours the use of the same in optical applications as a component.

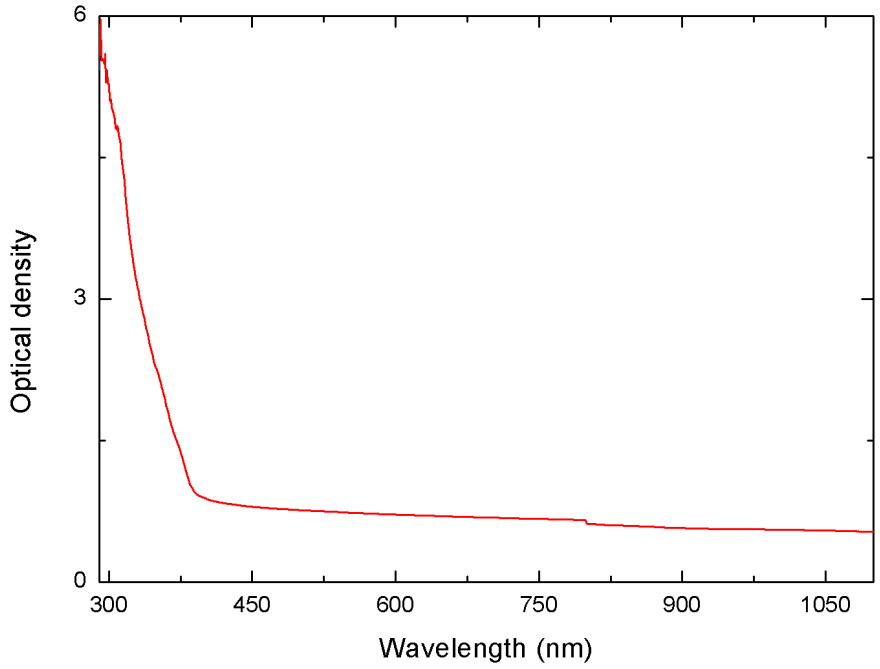

Figure 7. Absorption spectrum obtained in a pure resin sample with a thickness of 2.9 mm.

On the other hand, emission spectrum of the pure resin sample was obtained using the setup of Fig. 4 exciting at 405 nm and it is displayed in Fig. 8. It has a maximum peak at 500 nm, and a slow decrease of the emission intensity until approximately 900 nm.

The phenomenon of resin fluorescence causes that, in the applications of luminescence techniques on archaeological samples studies, the emission of bones or coprolites coexists with that of the resin, being difficult to distinguish one from the other. This fact makes that the manufacture of another type of chemical compound to prepare the archaeological samples to study, that does not produce fluorescence, is an investigation of importance for the application of this type of techniques.

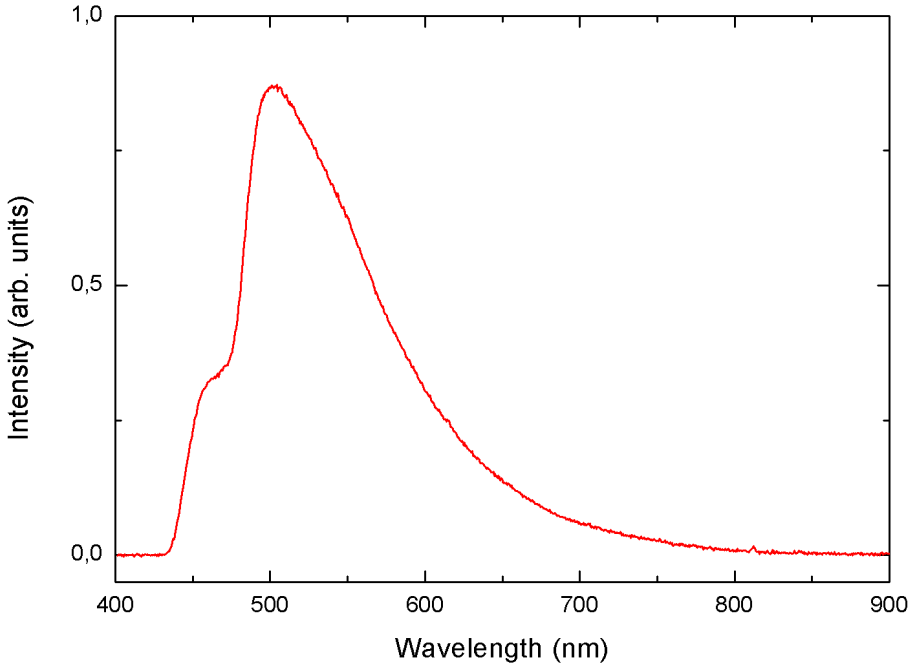

Figure 8. Emission spectrum obtained in a pure resin sample exciting at 405 nm.

5.2 COMPARISON OF THE EMISSION SPECTRA AND AVERAGE LIFETIMES OBTAINED IN REFERENCE SAMPLES

Reference sample bones spectra were measured using Fig. 4 setup, exciting with a 405 nm laser. With the aim of eliminate the resin fluorescence emission, a subtraction process was carried out, as it is exposed in Fig. 9. In first place, it was measured a spectrum exciting with the laser in the bone part of the sample. Then, a second spectrum was measured, but at this time the resin part of the sample was excited with the laser beam. Finally, the two spectra were subtracted after being normalized at 440 nm, thus eliminating the resin emission from the curves. The normalization at 440 nm is due to the fact that, after performing several tests, it is the one that does not produce negative values after the subtraction of the spectra. The results are shown in Fig. 10. For a better comparison, the spectra were normalized to their maximum value.

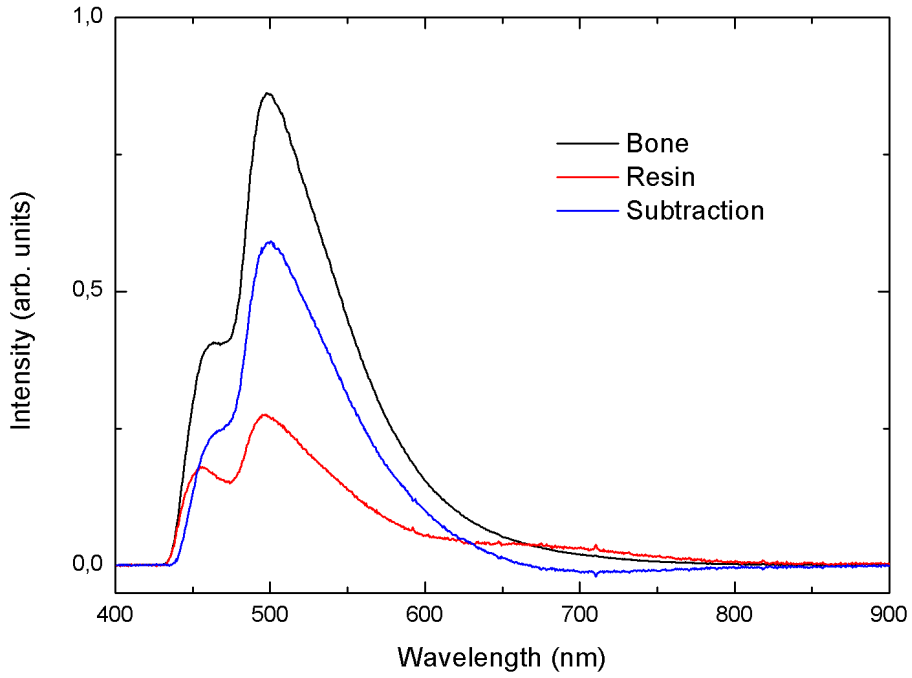

Figure 9. Subtraction process in reference bones samples. Emission spectra of a reference bone (black), resin (red) and spectrum obtained from the subtraction process (blue).

The measured spectra are in concordance with previous results in other works. As can be seen, the spectral curves obtained are similar to those shown in Fig. 2, where it is visible that bone samples fluorescence is mainly due to hydroxyapatite, in addition to collagen.

Despite of the similarity of most spectra, a small shift in the goat tibia sample and a softer descent at larger wavelengths is easily identifiable. In addition, the emission intensity in this example decreases significantly with respect to the rest, being visible in the graph due to the signal-to-noise ratio. On the other hand, it is recognizable in the ancient human tibia sample a softer decay towards longer wavelengths than in the modern one.

An important point to care about it is that, after the laser has excited the bone, it is reflected many times inside the glass and, as consequence, the resin of the sample is

excited. Due this circumstance, despite focusing laser emission on the bone of the specimen, the emission spectrum includes an overlap of both emissions.

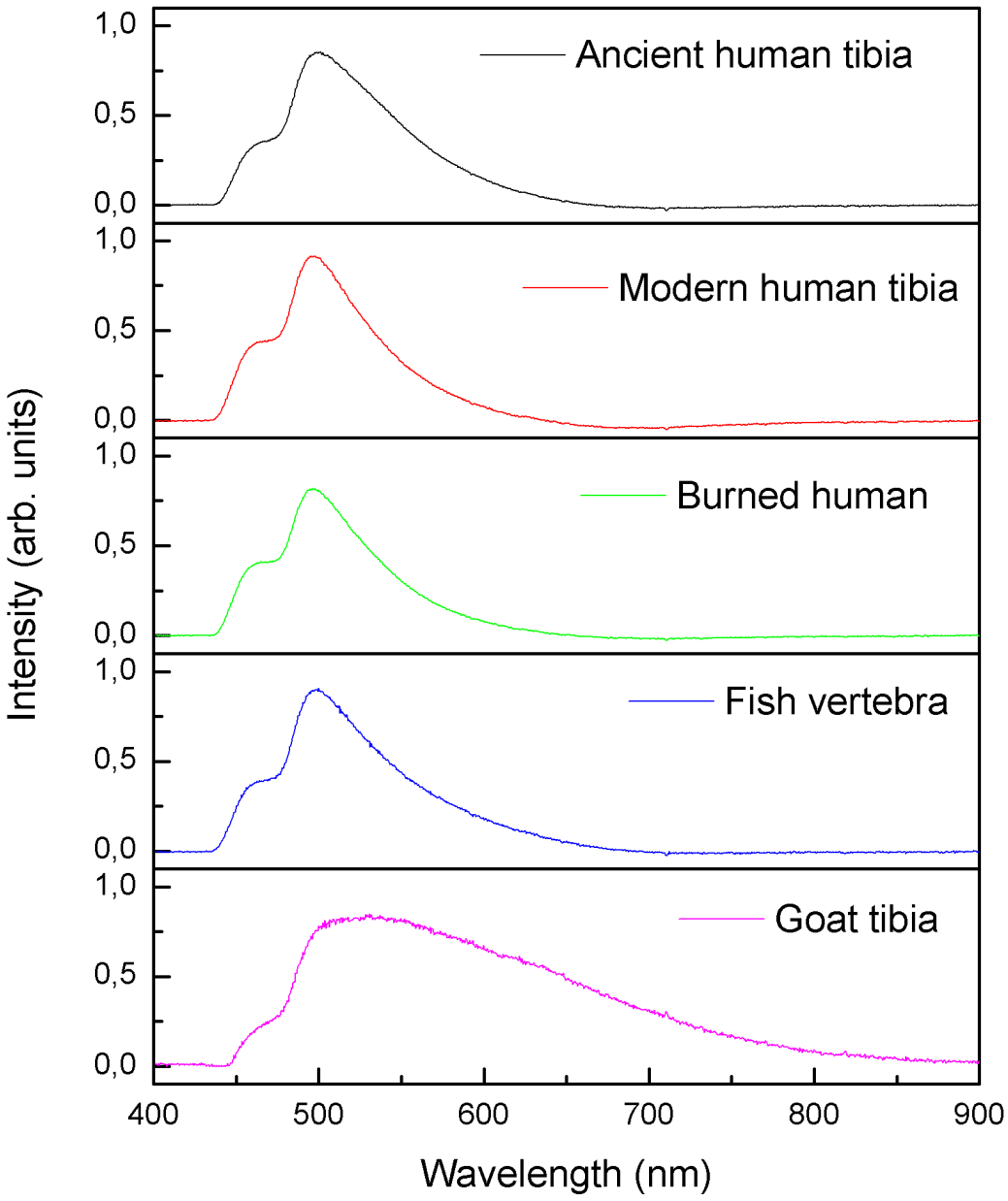

Figure 10. Reference bone samples emission spectra. The curves are normalized to their maximum value. The excitation source is at 405 nm.

Time resolved experiments have been carried out in order to detect differences among the different samples. The decay curves of the different samples were obtained exciting with a picosecond laser at 375 nm and detecting at 512 nm. As example, in Fig. 11 are shown the decay curves obtained in the ancient human tibia and in the goat tibia reference samples. As can be seen, there are important differences between these decays curves that have an important non exponential character.

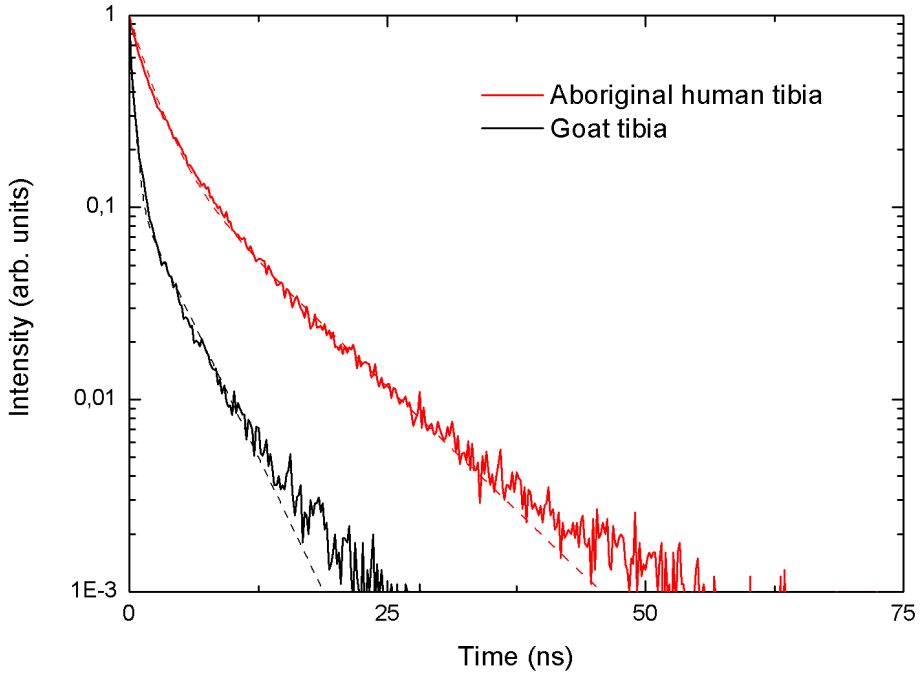

Figure 11. Decay curves of ancient human tibia (black) and goat tibia (red) samples. Double-exponential fits are also included (dashed lines).

With the aim to compare all the experimental decay curves obtained in the reference bones samples the results have been fitted to a double exponential decay. Using IRF reconvolution analysis with FAST software [12] have been obtained the average lifetimes using equation Eq. (11). The results are expressed in Table 1.

Table 1. Average lifetime of reference bone samples obtained exciting at 375 nm and detecting at 512 nm and using Eq. (11).

Sample name	B_1	B_2	τ_1 (ns)	τ_2 (ns)	τ_{av} (ns)
Ancient human tibia	1	0.12	2.07	8.44	4.18
Modern human tibia	1	0.08	1.66	7.23	3.16
Burned human	1	0.13	2.34	8.54	4.32
Fish vertebra	1	0.08	1.26	6.54	2.83
Goat tibia	1	0.04	0.38	3.91	1.44

Comparing the obtained values, a longer average lifetime is identifiable for the case of human bones, while the value that goes further away from the rest is that of the goat's bone. Moreover, in this sample its characteristic emission curve differs from the rest and has a lower intensity (see Fig. 10). This result can explain its low average lifetime.

Emission spectra of reference archaeological coprolites were measured using the same setup, and the results are displayed in Fig. 12.

Unlike previous results, some samples of coprolites have characteristics that differ markedly with the rest. The camel, cow and rabbit specimens present a characteristic peak ranging between 630 and 670 nm. It is especially striking that only herbivorous animals show this similarity, being possible to distinguish these sample with respect to the samples of omnivorous and carnivorous.

On the other hand, the pig coprolite sample shows a displacement of its maximum up to 540 nm. It also has a much smoother decay than the rest of the samples to larger wavelengths. This suggests that “coprolite 06” sample is probably from a carnivorous animal.

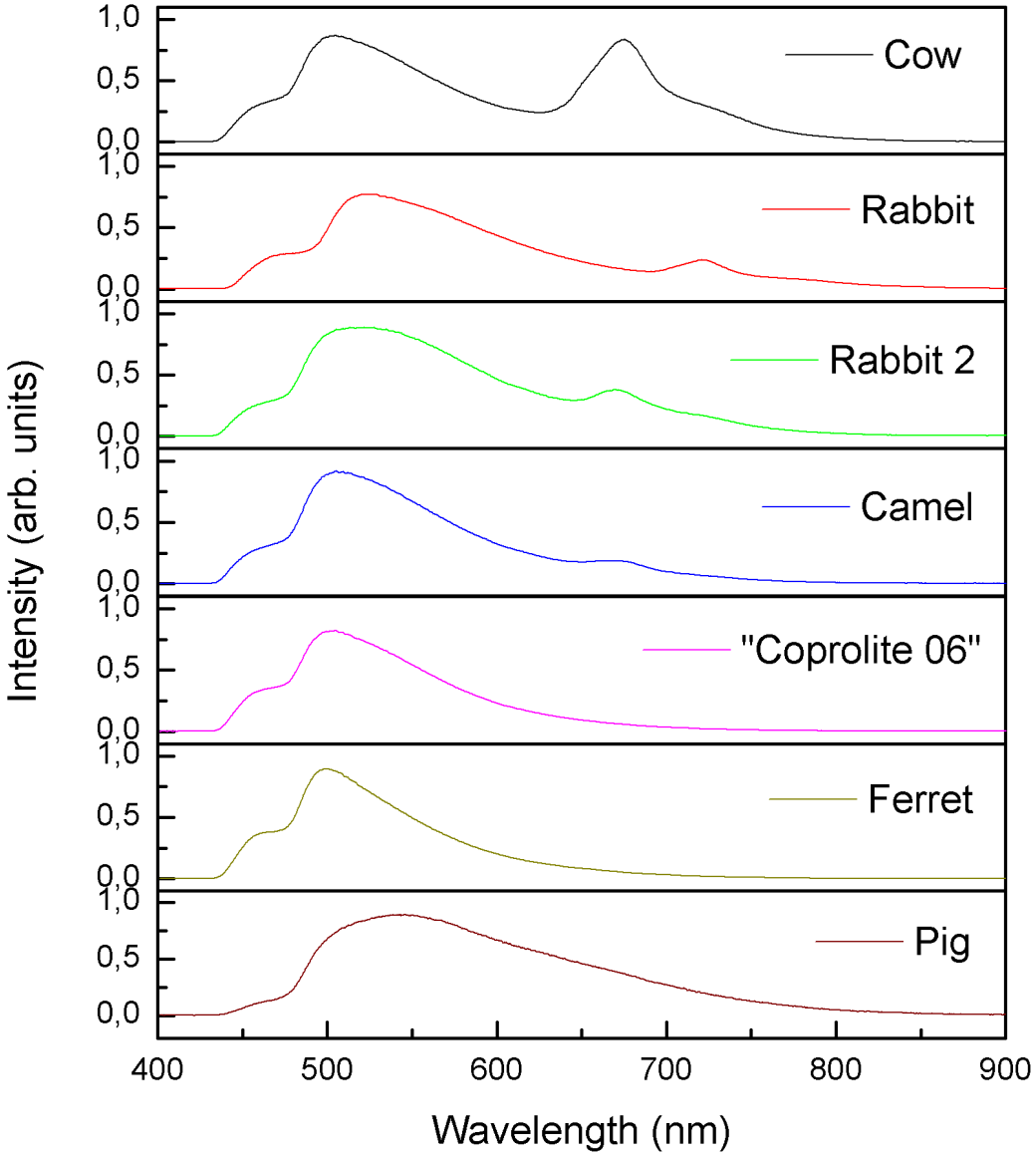

Figure 12. Emission spectra of reference coprolites samples. The curves are normalized to their maximum value. The excitation source is at 405 nm.

In the case of reference archaeological coprolites, the average lifetime values of herbivores specimens seem to be shorter than the rest (see Table 2). Moreover, these herbivores have different emission spectra. The highest value is measured for the case of ferret sample, while the samples of “coprolite 06” and pig have similar average lifetimes.

Table 2. Average lifetimes of coprolites samples obtained exciting at 375 nm and detecting at 512 nm and using Eq. (11).

Sample name	B_1	B_2	τ_1 (ns)	τ_2 (ns)	τ_{av} (ns)
Cow	1	0.16	0.76	4.99	2.94
Rabbit	1	0.20	0.83	4.81	2.98
Camel	1	0.15	0.70	4.77	2.78
“Coprolite 06”	1	0.19	0.87	5.59	3.45
Ferret	1	0.10	1.50	11.32	5.68
Pig	1	0.17	0.74	5.84	3.63

Finally, spectra of diverse reference samples were measured exciting with an OPO pulse laser at 380 nm. The emission spectra are shown in Fig. 13. Although in this range of excitation wavelengths the emission of bones and coprolites with respect to the resin is greater than in the previous case, it can be seen that the spectral distributions are very similar. This result is interesting because at this excitation wavelength is not necessary to make the subtraction process shown in Fig. 9.

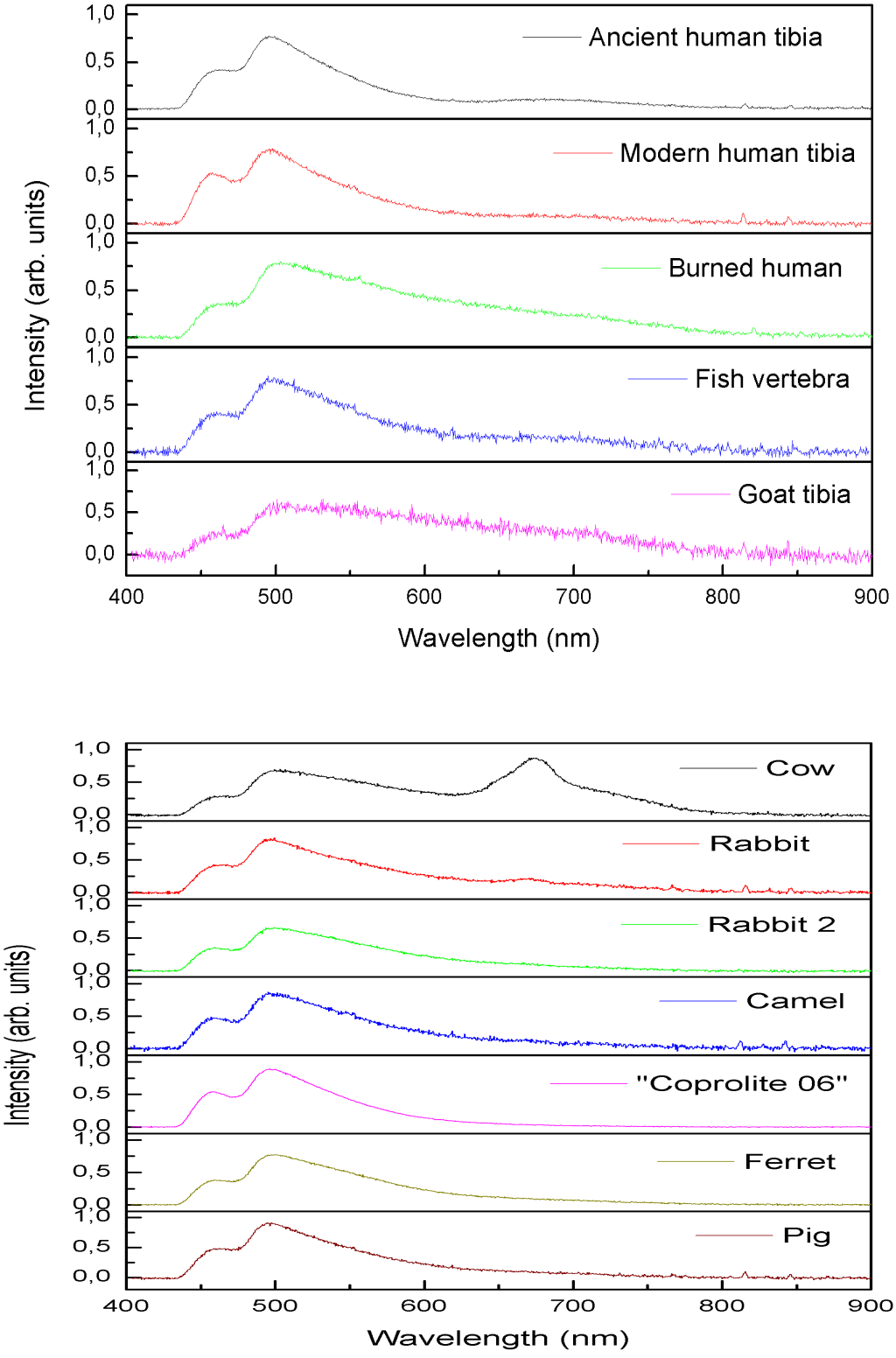

Figure 13. Emission spectra of reference samples exciting at 380 nm: top, bone samples; bottom, coprolites samples.

5.3 CHICKEN BONE EMISSION SPECTRA AND AVERAGE LIFETIMES AS A FUNCTION OF BURNING TEMPERATURE

Chicken bone emission spectra were obtained for calcination temperatures of 100, 200, 300 and 400° C. For this task, as in previous cases, the setup of Fig. 4 was used, exciting the sample at 405 nm laser. The emission spectra are shown in Fig. 14 and normalized to their maximum values.

In the non-calcinated sample, it is appreciable a maximum peak at 530 nm. In addition, diverse peaks distributed from 530 to 695 nm are perceptible, probably due to organic compounds present in the sample because it is still fresh. Moreover, a small shoulder at 460 nm is appreciable.

After heating the sample at 100° C, appreciable changes are shown in the emission curve. The spectrum is smoother and its maximum has been shifted to 520 nm. Probably at this treatment temperature the most of the organic compounds in the sample have been eliminated and only small peaks at 625 and 695 nm are appreciable. The 460 nm prominence is still recognised.

Emission spectrum of 200º C calcinated chicken sample is totally smooth, and centred at 520 nm. The previously existing organic compounds have been completely eliminated. However, the greatest change occurs after 300° C. The maximum emission is shifted towards 600 nm, in addition the emission intensity decreases significantly with respect to the previous ones, being the decreased signal-to-noise ratio observable in this curve. It seems reasonable to think that an important fluorescent component of the bone is lost at that temperature.

Finally, in the spectrum of the calcined sample at 400° C, a recovery of the relative emission intensity is observed and maximum displaces to 540 nm.

On the other hand, the analysis of the average lifetimes of the calcined chicken samples, shows a remarkable change in the values after 300° C (see Table 3). The average lifetimes decrease when the temperature is more than 300 ºC.

The important changes in the luminescence properties of the samples before and after the critical temperature of 300° C is in agreement with a previous FTIR study on burned bones [9], where it is observed that over this temperature there is a change in the chemical structure of the samples (see Table 4).

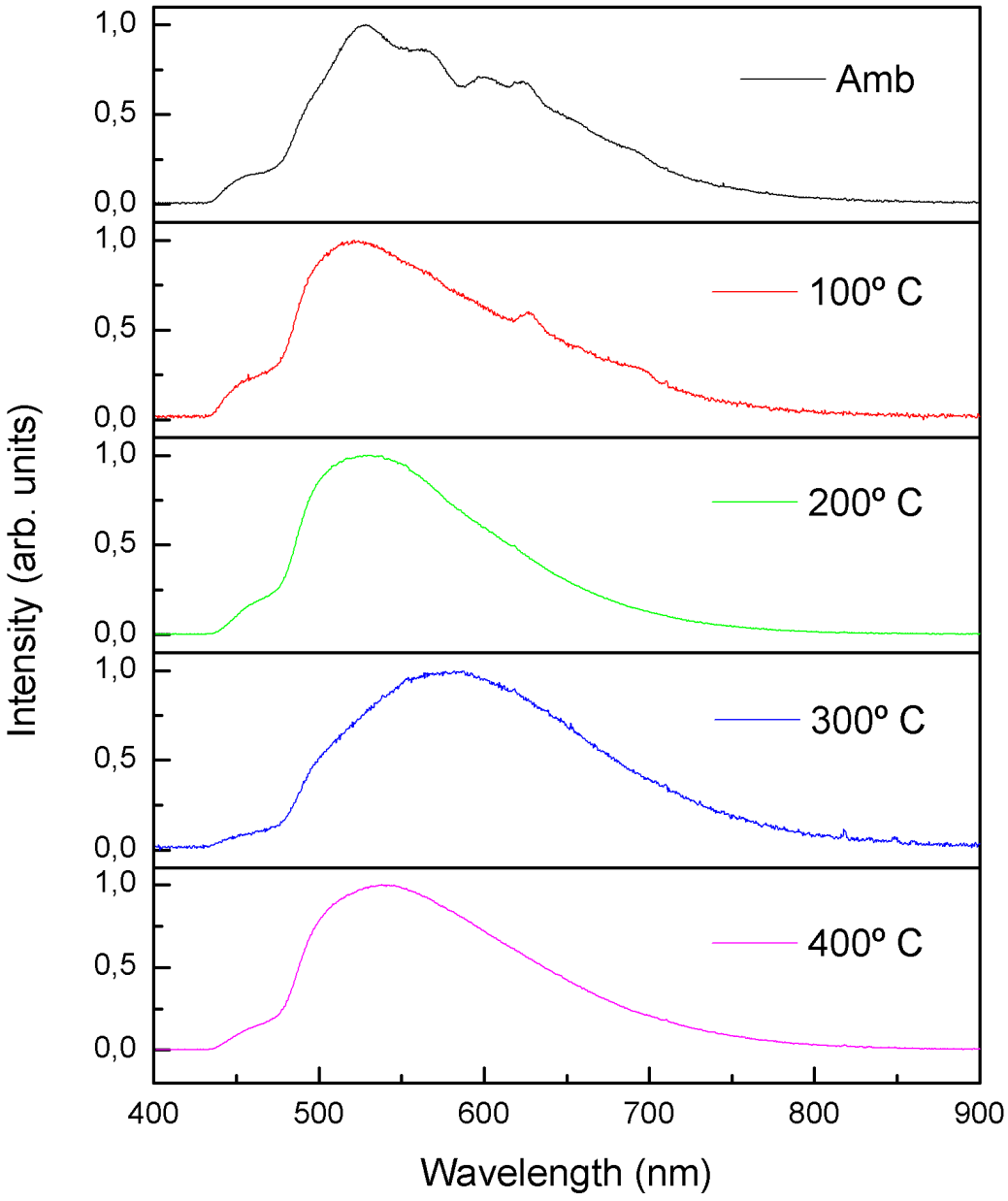

Figure 14. Emission spectra obtained in a chicken bone at ambient condition and at different burning temperatures. The curves are normalized to their maximum value and have been obtained exciting at 405 nm.

Table 3. Average lifetime of chicken burned samples exciting at 375 nm and detecting at 512 nm.

Sample name	B_1	B_2	τ_1 (ns)	τ_2 (ns)	τ_{av} (ns)
T=amb	1	0.33	3.28	9.87	6.57
T=100º C	1	0.37	3.17	9.55	6.53
T=200º C	1	0.18	3.37	10.85	6.09
T=300º C	1	0.06	1.74	9.48	3.57
T=400º C	1	0.11	2.18	7.70	3.70

Table 4. FTIR analyses of experimentally burned bones carried out in a previous study [9]. The table shows the loss of bone compounds at diverse temperatures. ✓= present, empty cell = absent, green = increase in absorption, red = decrease in absorption. (Table reproduced after Table 2 in [9]).

Assigned vibrational mode	Temperature (º C)								
	20	200	250	300	340	370	400	450	500
Amide A + B	√	√	√	√	√				
Amide I + II	√	√	√	√	√				
Amide III	√	√	√	√	√				
Amide IV–VII	√	√	√	√	√				
Aromatic compounds					√	√	√	√	√
Water (H_2O), adsorbed and structural	√	√	√	√	√	√	√	√	√
Splitting PO_4^{3-} v1 symmetric stretching	√	√	√	√	√	√	√	√	√
Splitting PO_4^{3-} v2 and v4 bending									
Change in PO_4^{3-} v3 peak width			√	√	√				
Shoulder on PO_4^{3-} v3 symmetric stretching									
Splitting PO_4^{3-} v4 bending (=SF)	√	√	√	√	√	√	√	√	√
CO_3^{2-} v2 / HPO_4^{2-} v2 (out of phase) bending	√	√	√	√	√	√	√	√	√
CO_3^{2-} v3 (a)symmetric stretching	√	√	√	√	√	√	√	√	√
New peak ~700 cm^{-1}									
New peak ~2020 cm^{-1}									

5.4 TIME RESOLVED SPECTROSCOPY

Time resolved spectroscopy techniques were used to analyse the cow coprolite sample. The obtained emission spectra as function of the delay time after the laser pulse excitation at 380 nm are shown in Fig. 15.

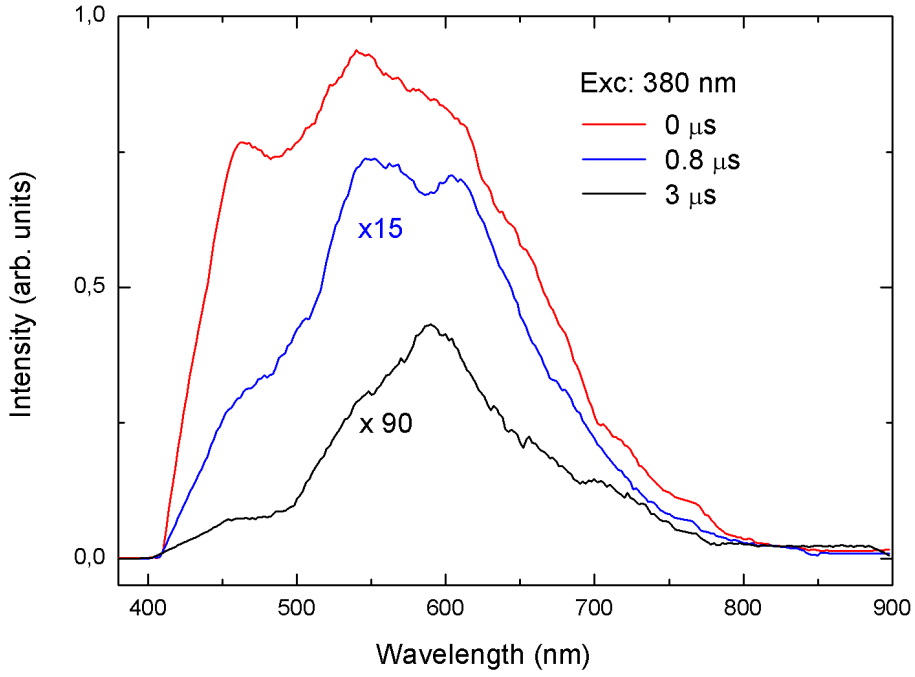

Figure 15. Emission spectra of cow coprolite sample measured using time resolved spectroscopy. Sample was excited using an OPO pulse laser at 380 nm. Blue curve is amplified 15 times, and black curve is amplified 90 times.

The red curve corresponds to the emission spectrum obtained immediately after the laser excitation with a temporal width of 200 ns. It has a peak about 460 nm and an absolute maximum at 540 nm. The blue curve corresponds to a delay of 0.8 μs after the sample excitation. In this spectrum, the shoulder about 460 has decreased and there is a red shift of the spectrum (centred at 600 nm). Finally, carrying out the measurement after 3 μs of the sample excitation has been obtained the emission spectrum shown in black in Fig. 15. Its intensity is very weak but the obtained emission band is clearly

centred at 600 nm. This peak characterizes the herbivores emission in Fig. 12 and it has been possible to isolate it using time resolve spectroscopy at long delay times.

The potential of the time resolved fluorescence technique is based on the ability to identify emission peaks from different physical processes that, initially being superimposed, has been possible to separate them. Therefore, in the application of luminescent techniques for the analysis of archaeological sediments, where fluorescent emission is a consequence of various chemical compounds, time resolved spectroscopy techniques seem to be a useful tool.

6 CONCLUSIONS

El análisis de los espectros de emisión de las muestras estándar de huesos y coprolitos sugiere que existen propiedades fluorescentes de muestras concretas que difieren del resto, a pesar de que la mayoría son similares en distribución, encontrándose el máximo de emisión en 520 nm. El estudio de los tiempos de vida de dichas muestras nos indica que es un importante método para identificar algunas de las mismas, siendo un análisis complementario al de los espectros de emisión. El estudio de diferentes temperaturas de combustión en el hueso de pollo reafirma la importancia de los efectos de calcinación en las muestras arqueológicas, siendo una temperatura de especial importancia 300º C. La aplicación de técnicas de espectroscopía resuelta en el tiempo muestra su potencialidad en el análisis de la fluorescencia de muestras arqueológicas.

In spite of having a good transparency, the absorption in the UV range and the fluorescence properties of the resin make the development of other types of resins essential for the luminescent analysis of archaeological sediments. In addition, it forces us to use a method capable of discerning between the luminescence of the same and the own of the bones or coprolites in archaeological sediments.

The study of the emission spectra of the reference bone samples, supplemented with the analysis of the lifetimes, indicates that some specimens show characteristic luminescent properties that can be used for the classification of the same. These spectra present in a majority a similar distribution, being the maximum emission centred at 520 nm.

On the other hand, the examination of the emission spectra of the reference samples of coprolites concludes that, in first stage, the specimens of herbivorous animals have a clear peak between 630 and 670 nm, being thus possible their identification with respect to the rest. The relative intensity of the same could also give us information about the diet of the animal. The obtained values of average lifetimes

reaffirm this intrinsic property of the samples, also showing a clear difference between the studied coprolites.

Finally, the application of time resolved spectroscopy technique demonstrates a clear importance on the archaeological analysis. The simultaneous existence of fluorescence emission of resin and bones or coprolites in prepared archaeological sediments is easily avoidable using this technique. The spectral curves measured using time resolved technique show a red-shift to 600 nm when the longest component of the decay curve is analysed, as opposed to the spectrum obtained at shorter delays, which has its maximum emission located at 540 nm.

6.1 OUTLOOK

In first place, the research must be extended to the study of more reference samples, with the aim to confirm the results obtained. In addition, it is necessary to develop a system that can adapt to the needs of the archaeological investigations, being of small size and light weight to be easily transported to the excavations and deposits, where an analysis of the recently extracted samples would be carried out.

A wide range of excitation wavelengths must be investigated in order to find the optimum configuration that maximizes the signal ratio between the emission of the resin and the sample itself.

On the other hand, higher calcination temperatures must be analysed, both near the critical temperature of 300° C, and temperatures above 400° C. These studies can be complemented with other characterization techniques such as TGA, DTA, DSC, FTIR, Raman spectroscopy or electron spectroscopy, which would facilitate information about variations in the structure of samples when treated with temperature

7 REFERENCES

1. Georges Stoops. “Guidelines for Analysis and Description of Soil and Regolith Thin Sections”. Soil Science Society of America (2003).
2. Georges Stoops, Vera Marcelino and Florias Mees. “Interpretation of Micromorphological Features of Soils and Regoliths”. Elsevier Science (2010).
3. H. -J Altemüller and B. Van Vliet-Lanoe. “Soil Thin Section Fluorescence Microscopy”. Developments in Soil Science, 19, 565-579 (1990).
4. Michael Gaft, Renata Reisfeld and Gerard Panczer. “Modern Luminescence Spectroscopy of Minerals and Materials”. Springer International Publishing Switzerland (2015).
5. Adrian P. Hunt, Spencer G. Lucas, Jesper Milàn and Justin A. Spielmann. “Vertebrate Coprolites”. New Mexico Museum of Natural History & Science, 57 (2012).
6. I Mayer, J.D. Layani, A. Givan, M. Gaft and Ph. Blanc. “La ions in precipitated hydroapatites”. Journal of Inorganic Biochemistry, 73, 221–226 (1999).
7. Ota Samek, Helmut H Telle and David CS Beddows. “Laser-induced breakdown spectroscopy: a tool for real-time, in vitro and in vivo identification of carious teeth”. BMC Oral Health, 1:1 (2001).
8. Hüseyin Toktamiş, Dilek Toktamiş, S. Merve Yilmaz, A. Necmeddin Yazici, Cihan Yildirim and Özlem Özbiçki. “The investigation of usage of fluorapatite mineral ($Ca_5F(PO_4)_3$) in tooth enamel under the different pre-irradiation thermal treatments”. Thermochimica Acta, 600, 102-109 (2014).
9. J. Roman-Lopez, V. Correcher, J. Garcia-Guinea, T. Rivera and I.B Lozano. “Thermal and electron stimulated luminescence of natural bones, commercial hydroxyapatite and collagen”. Spectrochimica Acta Part A: Molecular and Biomolecular Spectroscopy, 120, 610-615 (2013).
10. Femke H. Reidsma, Annelies van Hoesel, Bertil J. H. van os, Luc Megens and Freek Braadbaart. “Charred bone: Physical and chemical changes during laboratory simulated heating under reducing conditions and its relevance for the study of fire use in archaeology”. Journal of Archaeological Science: Reports, 10, 282-292 (2016).

11. S. Trujillo, P. Martínez-Torres, P. Quintana and Juan Jose Alvarado-Gil. “Phototermal Radiometry and Diffuse Reflectance Analysis of Thermally Treated Bones”. Int J Thermophys, 31, 805–815 (2010).
12. P. Martín-Ramos, M. Ramos Silva, F. Lahoz, I.R. Martín, P. Chamorro-Posada, M.E.S Eusebio, V. Lavín, J. Martín-Gil. “Highly fluorinated erbium (III) complexes for emission in the C-band”. Journal of Photochemistry and Photobiology A: Chemistry, 292, 16-25 (2014).
13. J.R. Lakowicz. “Principles of Fluorescence Spectroscopy”. Springer (2006).